

Nonlinear conductivity and noise spectrum of a pinned charge-density wave

L. Pietronero and S. Strässler*

Brown Boveri Research Center, CH-5405 Baden, Switzerland

(Received 4 May 1983)

We study the overdamped phase dynamics of a charge-density wave (CDW) pinned by randomly located impurities fully including the internal degrees of freedom of the CDW. The current-field behavior, the threshold field, and the phase diagram (pinned versus unpinned) are characterized and discussed. The narrow-band noise is computed explicitly for the full many-body problem, and it is found to be of the type observed in NbSe₃.

The unusual transport properties of NbSe₃ have been related to the two charge-density waves (CDW's) that appear below $T_1=145$ K and $T_2=59$ K.¹ This conclusion is due to the following results: Below T_1 and T_2 , an increase of resistivity is observed that manifests dielectric breakdown under the effect of an electric field.² Electric fields that strongly reduce the resistivity have no effect on the intensity or period of the CDW.³ A threshold electric field exists⁴ below which the CDW is pinned and the power spectrum of the current above this field shows a remarkable narrow band noise.⁴ The pinning is mainly due to impurities.⁵

Different models have been proposed to describe the depinning and dynamical properties of CDW's. The most common approach is to treat the CDW (or a portion of it) as a single classical particle that moves in a periodic potential.⁶ The motion is overdamped as shown by the frequency-dependent conductivity⁷ so the kinetic term is usually neglected. An alternative description is based on tunneling of portions of CDW's.⁸ Both approaches are supported by some of the available data but also show important discrepancies.^{9,10}

In the present paper we characterize and discuss the properties of the *true classical model*. We study the overdamped phase dynamics of a CDW pinned by randomly located impurities fully including its internal degrees of freedom. Results are presented for the current-field behavior, the threshold field and the (pinned versus unpinned) phase diagram. We also compute explicitly the narrow-band noise for the full many-body problem and this results to be of the type observed in NbSe₃. Some contradictory numerical results for models related to the present one have been reported^{11,12} and when possible will be compared to our results. The variational approach for the weak pinning region¹³ will be also discussed. Even if the CDW dynamics in NbSe₃ shows some three-dimensional correlation¹⁰⁻¹³ the model we study is purely one-dimensional because it is more suitable for numerical treatments and with proper interpretation can give important clues on the analysis of the experiments.

We consider the phase modes of a CDW at $T=0$ K. The CDW is assumed of the form

$$\rho(x) = e\rho_0\{1 + C \cos[q_0x + \phi(x)]\}, \quad (1)$$

where ρ_0 is the one-dimensional electron density (e is the

electron charge) and $l=2\pi/q_0$ is the wavelength of the CDW. The phase $\phi(x)$ denotes the position of the CDW.

In a Peierls system with a constant density of states per site N_0 there results $C=N_0\Delta/a\lambda\rho_0$ (Ref. 14) where a is the lattice constant, 2Δ is the gap, and λ is the electron-phonon coupling. Neglecting the kinetic term^{6,7} (overdamped motion) the energy density is

$$U = \frac{K}{2q_0^2} \left(\frac{\partial\phi}{\partial x} \right)^2 - \frac{e\rho_0}{q_0} \phi E + V_0 \sum_j \rho(x)\delta(x-x_j). \quad (2)$$

The first term in Eq. (2) represents the elastic energy of the CDW, for a Peierls system $K=\rho_0mv_F^2$ (Refs. 15 and 16) where m is the free-electron mass and v_F is the Fermi velocity. The second term couples the electric field E to the CDW. The third term represents the interaction energy with impurities located at random positions x_j and acting only at these positions. V_0 is the intensity of this interaction and the index j runs over the impurities whose density is n_i . To the equation of motion corresponding to Eq. (2) we add a damping force F_d acting only at the impurity positions

$$F_d = -\frac{\rho_m}{q_0^2\tau} \sum_j \dot{\phi}(x)\delta(x-x_j), \quad (3)$$

where ρ_m is the effective-mass density of the CDW, τ is a phenomenological parameter that characterizes the dissipation of energy from the moving CDW to the lattice, and the dot indicates time differentiation. This assumption for how damping acts on the CDW is plausible and gives rise to important computational simplifications. The total equation of motion is

$$-\frac{K}{q_0^2} \frac{\partial^2\phi}{\partial x^2} - \frac{\rho_m}{q_0^2\tau} \sum_j \dot{\phi}(x)\delta(x-x_j) + e\rho_0CV_0 \sum_j \sin[q_0x_j + \phi(x)]\delta(x-x_j) + \frac{e\rho_0}{q_0} E = 0. \quad (4)$$

It is convenient to introduce the following dimensionless variables. For the distance $u=n_ix$, for the field $\xi=E/E_0$ where $E_0=CV_0n_iq_0$, for the elastic constant $B=2\pi Kn_i/CeV_0\rho_0q_0^2$, for the time $s=t/\tau_0$ where $\tau_0=2\pi\rho_m n_i^2/CeV_0\rho_0q_0^2\tau$. For the phase at an impurity

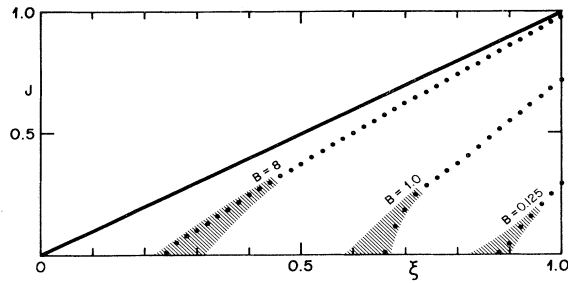


FIG. 1. Current (J) vs normalized field (ξ) relation for different values of the coupling B . See Eq. (5). The dots refer to a case with $N=80$ impurities. The shaded areas represent the typical fluctuations due to different N (with fixed density n_i) and to different realizations of the random distribution for the impurities [see text at the point (i)]. The continuous line represents the asymptotic behavior for large ξ to which the plotted J is normalized.

site $\psi_j = \phi(x_j)/2\pi$. Furthermore, we introduce $Q_0 = q_0/2\pi n_i$.

The equation of motion [Eq. (4)] can be integrated exactly between any two subsequent impurities¹⁴ [this is the advantage of having the damping in the form given by Eq. (3)] and reduces to a difference equation that only involves the phases ψ_j at each impurity site. With the new variables just introduced we have then simply

$$\frac{d\psi_j}{ds} = B \left[\frac{\psi_{j+1} - \psi_j}{r_{j+1,j}} - \frac{\psi_j - \psi_{j-1}}{r_{j,j-1}} \right] - \sin[2\pi(u_j Q_0 + \psi_j)] + \xi Q_j, \quad (5)$$

where $r_{j+1,j} = u_{j+1} - u_j$ is the normalized distance between two subsequent impurities and $Q_j = \frac{1}{2}(r_{j+1,j} + r_{j,j-1})$ can be considered as the effective charge associated with the impurity at position j . In terms of the ψ_j 's the current density is given by

$$J = en_e \frac{2\pi}{q_0 \tau_0} \left\langle \frac{d\psi_j}{ds} Q_j \right\rangle, \quad (6)$$

where n_e is the bulk electron density and $\langle \rangle$ represents an average over all impurity sites. Equation (5) has been solved numerically with cyclic boundary conditions. The number of impurities has been varied normally between 1 and 1000 but a few runs, up to 5000, have been made to check convergency. The position of the impurities has been assumed to be random (Poisson distribution) and the strength of their potential equal for all. The results can be summarized as follows:

(i) *Polarization, threshold field ξ_{th} and $J(\xi)$ relation.* The threshold field ξ_{th} is defined by the maximum value of ξ for which Eq. (5) has solution $d\psi_j/ds=0$. In studying this question numerically caution has to be taken for the following problem. Given a system relaxed into a stable configuration and applying a field ξ it often hap-

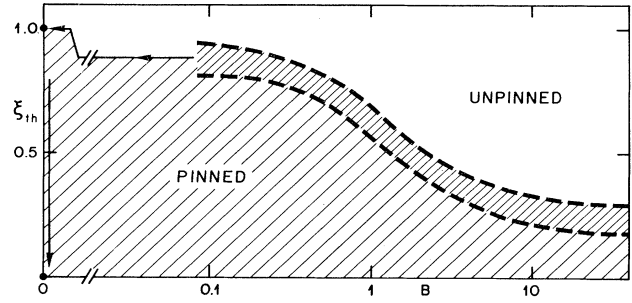


FIG. 2. Pinned vs unpinned phase diagram. We show here the dependence of the (normalized) threshold field ξ_{th} on the coupling B [see Eq. (5)]. The limit of large B (weak pinning) can be reasonably described by $\xi_{th} \sim B^{-1/3}$ that arises from the variational approach. For $B \sim 0$ the behavior of ξ_{th} is nonanalytic. See point (ii).

pens that the system evolves into a new configuration and afterwards it stops. This phenomenon of nonlinear polarization (that also produces an hysteresis) gives rise to $d\psi_j/ds \neq 0$ for some finite time interval but it should not be confused with the onset of a current in the system. This produces some complications in defining ξ_{th} starting from low fields because the current has to be averaged over a long time. The problem can be avoided by starting at large ξ and defining ξ_{th} as the value at which the current becomes zero. In Fig. 1 we report some examples of current (J) versus field (ξ) behavior. The current is normalized with respect to its asymptotic behavior. For each value of the coupling B we have varied the number of impurities N and also considered different configurations for the random impurities. The dots refer to a particular case with $N=80$ and the shaded areas indicate the typical fluctuations due to different values of N (from 20 to 1000) and to different realizations of the random distribution. No appreciable monotonic behavior is observed for ξ_{th} as a function of N . Our results indicate, therefore, that ξ_{th} should remain finite for $N \rightarrow \infty$. This is in agreement with Ref. 12 and in contrast to Ref. 11. The results (Fig. 1) also indicate that the singularity of $dJ/d\xi$ at ξ_{th} present in the single-particle model disappears for our system or at least is confined to a very narrow region. The best "sample" we have considered (large N , long-time average, and starting from large ξ) seem to indicate that the current starts as $J \sim \xi - \xi_{th}$. This behavior should not be too sensitive to the effect of some $3d$ coupling and it is in good agreement with preliminary low-temperature ($T \sim 4$ K) data.¹⁷

(ii) *Dependence of ξ_{th} on B . Pinned versus unpinned phase diagram.* The threshold field ξ_{th} is only a function of the parameter B introduced after Eq. (4). This dependence is shown in Fig. 2 and it is in qualitative agreement with Fig. 5 of Ref. 11. In the limit of large B (weak pinning) using the variational approach of Ref. 13 one obtains $\xi_{th} \sim B^{-1/3}$ (to which corresponds $E_{th} = E_0 \xi_{th} \sim n_i^{2/3}$) in reasonable agreement with the numerical results of Fig. 2. For a three-dimensional case one has instead $\xi_{th} \sim B$

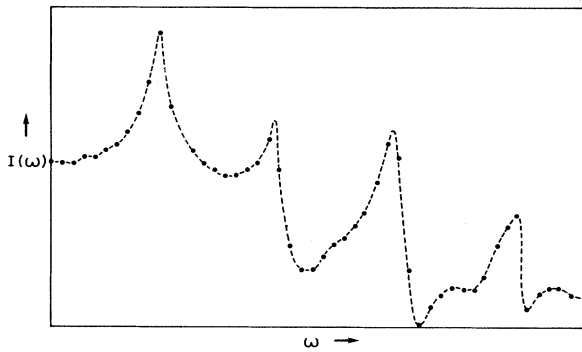


FIG. 3. Example of narrow-band noise above ξ_{th} for a system with $N=40$, $B=10$, $\xi=1$. The power spectrum (plotted as a function of the frequency in arbitrary units) can be interpreted along the skeleton of the single-particle model. See point (iii).

and $E_{th} \sim n_i^2$.

In the limit $B \rightarrow 0$ (strong pinning) there is a problem of nonanalyticity because for $B=0$ the CDW splits into independent portions of different lengths each pinned by an

impurity. This corresponds mathematically to many domains with a distribution of pinning energies¹⁰ and produces a long tail in $J(\xi)$ so that $\xi_{th}=0$. For any small (but finite) value of B the CDW portions cannot really decouple and the threshold field is large ($\xi_{th} \rightarrow 1$).

(iii) *Narrow-band noise.* We have investigated numerically the noise spectrum corresponding to the dynamics of the CDW above ξ_{th} and an example is reported in Fig. 3 for the case $B=10$, $\xi=1$, and $N=40$. The noise intensity plotted is $I(\omega) = \log_{10}[|J(\omega)|^2]$ where $J(\omega)$ is the Fourier transform of $J(s)$ (s is a dimension time unit). This noise spectrum peaks at frequencies $\omega_n \sim nJ/l$ ($n=1,2,\dots$) and can be interpreted along the skeleton given by the single-particle picture.⁶ This shows that the complete field description for the CDW also gives rise to a narrow-band noise of the type of that observed experimentally.⁴

ACKNOWLEDGMENTS

The authors are grateful to G. Grüner and P. Monceau for interesting discussions.

*Present address: Cerberus AG, CH-8708 Männedorf, Switzerland.

¹Proceedings of the International Conference on Low-Dimensional Conductors, Part C, edited by A. J. Epstein and E. M. Conwell [Mol. Cryst. Liq. Cryst. **81**, Nos. 1–4 (1982)].

²P. Monceau, N. P. Ong, A. M. Portis, A. Meershaut, and J. Rouxel, Phys. Rev. Lett. **37**, 602 (1976); N. P. Ong and P. Monceau, Phys. Rev. B **16**, 3443 (1977).

³R. M. Fleming, D. E. Moncton, and D. B. McWhan, Phys. Rev. B **18**, 5560 (1978).

⁴R. M. Fleming and C. C. Grimes, Phys. Rev. Lett. **42**, 1423 (1979).

⁵N. P. Ong, J. W. Brill, J. C. Eckert, J. W. Savage, S. K. Khanna, and R. B. Somoano, Phys. Rev. Lett. **42**, 811 (1979); Phys. Rev. B **23**, 1517 (1981).

⁶G. Grüner, A. Zawadowski, and P. M. Chaikin, Phys. Rev. Lett. **46**, 511 (1981).

⁷G. Grüner, L. C. Tippie, J. Sanny, W. G. Clark, and N. P. Ong, Phys. Rev. Lett. **45**, 935 (1980).

⁸J. Bardeen, Phys. Rev. Lett. **42**, 1498 (1979); **45**, 1978 (1980).

⁹G. Grüner, A. Zettl, W. G. Clark, and J. Bardeen, Phys. Rev. B **24**, 7247 (1981).

¹⁰P. Monceau, J. Richard, and M. Renard, Phys. Rev. B **25**, 931 (1982); **25**, 948 (1982).

¹¹N. Teranishi and R. Kubo, J. Phys. Soc. Jpn. **47**, 720 (1979).

¹²J. B. Sokoloff, Phys. Rev. B **23**, 1992 (1981).

¹³P. A. Lee and T. M. Rice, Phys. Rev. B **19**, 3970 (1979); T. M. Rice, Festkörperprobleme **XX**, 393 (1980); A. M. Portis, in Proceedings of the International Conference on Low-Dimensional Semiconductors, Part C, Ref. 1, p. 777. For a study of linear-response properties see H. Fukuyama and P. A. Lee, Phys. Rev. B **17**, 535 (1978).

¹⁴L. Pietronero and S. Strässler (unpublished).

¹⁵P. A. Lee, T. M. Rice, and P. W. Anderson, Solid State Commun. **14**, 703 (1974).

¹⁶L. Pietronero, S. Strässler, and G. A. Toombs, Phys. Rev. B **12**, 5213 (1975).

¹⁷G. Grüner (unpublished).